

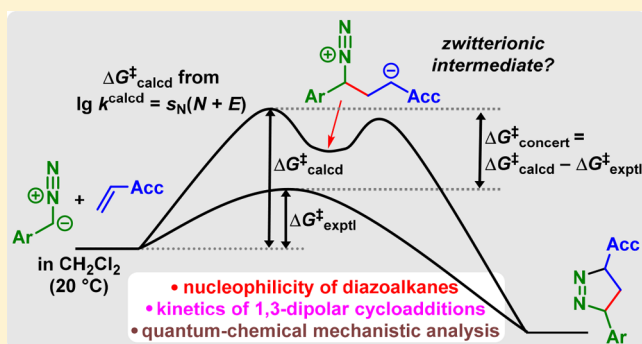
Nucleophilicity and Electrophilicity Parameters for Predicting Absolute Rate Constants of Highly Asynchronous 1,3-Dipolar Cycloadditions of Aryldiazomethanes

Harish Jangra,[†] Quan Chen,^{†,‡} Elina Fuks,^{†,§} Ivo Zenz,[§] Peter Mayer,[‡] Armin R. Ofial,^{*†§} Hendrik Zipse,^{*†§} and Herbert Mayr^{*†§}

Department Chemie, Ludwig-Maximilians-Universität München, Butenandtstr. 5-13, 81377 München, Germany

Supporting Information

ABSTRACT: Kinetics of the reactions of aryldiazomethanes (ArCHN_2) with benzhydrylium ions (Ar_2CH^+) have been measured photometrically in dichloromethane. The resulting second-order rate constants correlate linearly with the electrophilicities E of the benzhydrylium ions which allowed us to use the correlation $\lg k = s_N(N + E)$ (eq 1) for determining the nucleophile-specific parameters N and s_N of the diazo compounds. UV–vis spectroscopy was analogously employed to measure the rates of the 1,3-dipolar cycloadditions of these aryldiazomethanes with acceptor-substituted ethylenes of known electrophilicities E . The measured rate constants for the reactions of the diazoalkanes with highly electrophilic Michael acceptors ($E > -11$, for example 2-benzylidene Meldrum's acid or 1,1-bis(phenylsulfonyl)ethylene) agreed with those calculated by eq 1 from the one-bond nucleophilicities N and s_N of the diazo compounds and the one-bond electrophilicities of the dipolarophiles, indicating that the incremental approach of eq 1 may also be applied to predict the rates of highly asynchronous cycloadditions. Weaker electrophiles, e.g., methyl acrylate, react faster than calculated from E , N , and s_N , and the ratio of experimental to calculated rate constants was suggested to be a measure for the energy of concert $\Delta G_{\text{concert}}^\ddagger = RT \ln(k_2^{\text{exptl}}/k_2^{\text{calcd}})$. Quantum chemical calculations indicated that all products isolated from the reactions of the aryldiazomethanes with acceptor substituted ethylenes (Δ^2 -pyrazolines, cyclopropanes, and substituted ethylenes) arise from intermediate Δ^1 -pyrazolines, which are formed through concerted 1,3-dipolar cycloadditions with transition states, in which the C–N bond formation lags behind the C–C bond formation. The Gibbs activation energies for these cycloadditions calculated at the PCM(UA0,CH₂Cl₂)/(U)B3LYP-D3/6-31+G(d,p) level of theory agree within 5 kJ mol⁻¹ with the experimental numbers showing the suitability of the applied polarizable continuum model (PCM) for considering solvation.



INTRODUCTION

1,3-Dipolar cycloadditions (Huisgen reactions) represent the most general approach to 5-membered heterocycles.¹ They have been used for the total synthesis of natural products² and for the preparation of organic functional materials.³ The copper-catalyzed reaction of azides (R-N_3) with alkynes has become the most generally applicable click reaction.⁴ Although a concerted mechanism with a cyclic transition state has been well established for most Huisgen reactions,^{5–7} evidence for a stepwise course via diradical or zwitterionic intermediates has been reported in several cases.^{6,8} Since the late 1970s, reactivities and regioselectivities of cycloaddition reactions have commonly been interpreted on the basis of perturbational molecular orbital theory.^{7,9} Recently, the groups of Houk and Bickelhaupt have shown that detailed insight in the mechanisms of these reactions can be obtained by the “distortion/interaction energy” or “activation strain” model, respectively.^{10–12} We now report a novel approach to

predicting and analyzing cycloaddition reactivities on the basis of linear-free-energy relationships.

Equation 1, in which nucleophiles are characterized by two solvent-dependent parameters, N and s_N , and electrophiles are characterized by one parameter, E , has been demonstrated to predict rate constants of a large variety of electrophile-nucleophile combinations if one or both reaction centers are carbon.^{13,14}

$$\lg k_{20^\circ\text{C}} = s_N(N + E) \quad (1)$$

While the electrophilicity parameter E of a certain electrophile is derived from the rate constants of its reactions with a series of C-centered nucleophiles, the N and s_N parameters of a certain nucleophile are derived from the rates of its reactions with a series of C-centered reference electrophiles. Since

Received: September 14, 2018

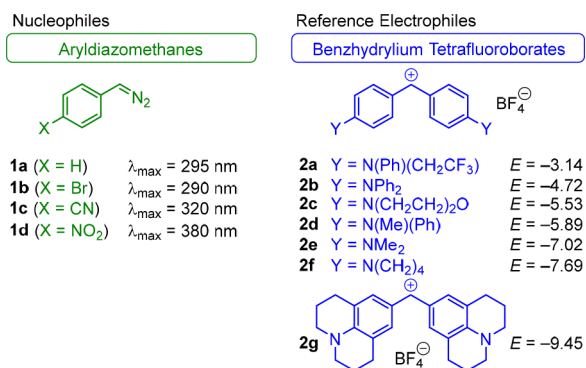
reactions, in which *one* and only *one* new bond is formed in the rate-determining step, were used for the derivation of the reactivity parameters E , N , and s_N , eq 1 cannot be expected to be applicable to multicenter processes. However, we now report that the relative reactivities of Michael acceptors toward aryldiazomethanes¹⁵ correlate well with the electrophilicities E of Michael acceptors, which have previously been derived from the one-bond reactivities of the electron-deficient π -systems toward carbanions and ylides.¹⁶ We will furthermore show that eq 1 can even be used to predict absolute rate constants for the reactions of highly electrophilic dipolarophiles with aryldiazomethanes, whereas less electrophilic dipolarophiles react faster than predicted by eq 1 due to the concerted formation of two new σ -bonds. In the latter cases, deviations of the measured cycloaddition rate constants from those calculated by eq 1 can be considered to be a measure for the energy of concert $\Delta G_{\text{concert}}^\ddagger$, as defined in eq 2.¹⁷

$$\Delta G_{\text{concert}}^\ddagger = RT \ln(k_2^{\text{exptl}}/k_2^{\text{calcd}}) \quad (2)$$

RESULTS AND DISCUSSION

Phenyldiazomethane **1a** and its *para*-substituted derivatives **1b–d**, which have UV absorption maxima between 290 and 380 nm, were employed for this study (Chart 1). For the

Chart 1. Aryldiazomethanes (**1**) and Benzhydrylium Tetrafluoroborates (**2-BF₄**) Used in This Work

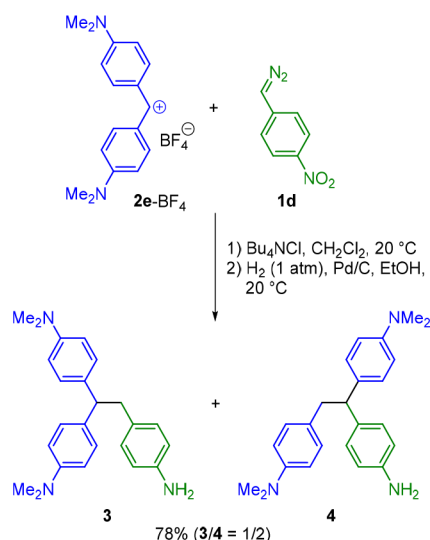


determination of the reactivity parameters N and s_N for **1a–d** the rates of their reactions with a set of colored benzhydrylium ions of known electrophilicities $E^{13a,h}$ (**2a–g** in Chart 1) were measured.

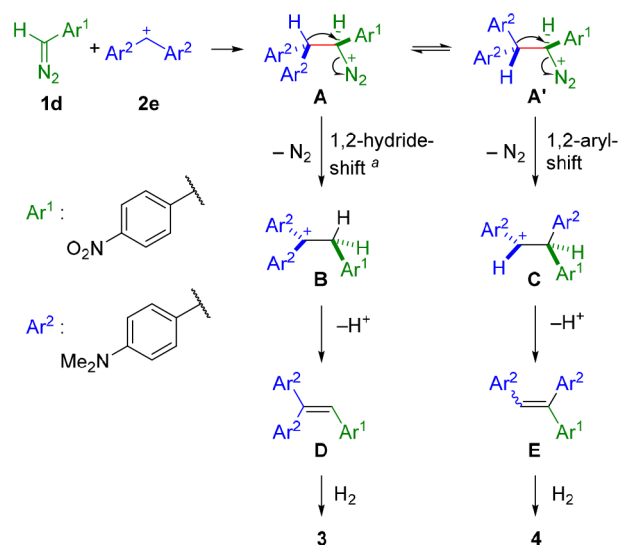
Determination of Nucleophile-Specific Parameters N and s_N for Aryldiazomethanes **1b–d.**¹⁸ *Product Studies.* The reaction of **1d** with **2e** gave a mixture of (*E*)- and (*Z*)-configured ethylenes, which was hydrogenated to furnish **3** and **4** in a 1:2 ratio and 78% yield of isolated products (Scheme 1).

The mechanism for their formation is rationalized in Scheme 2. The reaction between **1d** and **2e** yields a diazonium ion **A**, which spontaneously loses N₂ accompanied by a hydride shift, leading to carbenium ion **B**, or an aryl shift, leading to carbenium ion **C**. Deprotonation yields the olefins **D** and **E**, respectively, the precursors of the isolated products **3** and **4**. Alternatively, the nonrearranged olefin **D** may be formed by concerted proton and N₂ elimination from diazonium ion **A**. From the 3/4 ratio one can derive that the aryl shift is faster than the competing processes. Concerted N₂ departure and 1,2-shifts have previously been observed from diazonium ions

Scheme 1. Reaction of Aryldiazomethane **1d** with Benzhydrylium Tetrafluoroborate **2e-BF₄**



Scheme 2. Proposed Mechanism for the Formation of **3** and **4**



^aFormal hydride shift, which may include further intermediates.

generated by diazotation of primary amines¹⁹ as well as in acid-catalyzed Schmidt reactions of alkyl azides.²⁰

Kinetics. The rates of the reactions of the diazomethanes **1** with the benzhydrylium ions **2** were followed photometrically under pseudo-first-order conditions by monitoring the decay of the UV–vis absorbance of **2** in the presence of a large excess of **1**, following the procedure reported previously.¹⁸ The resulting second-order rate constants k_2 for the reactions between aryldiazomethanes **1** and benzhydrylium ions **2**, which correspond to the slopes of the plots of the pseudo-first-order rate constants k_{obs} vs $[1]$, are listed in Table 1. Linear correlations between $\lg k_2$ and the electrophilicity parameters E of **2** (Figure 1) indicate the applicability of eq 1. The slopes of the correlation lines and the negative intercepts on the abscissa correspond to the nucleophilicity parameters s_N and N , respectively, of **1** (Table 1).

The second-order rate constants for the reactions of **2e-BF₄** with the aryldiazomethanes listed in Table 1 correlate linearly

Table 1. Second-Order Rate Constants k_2^{exptl} for the Reactions of the Aryldiazomethanes **1 with Benzhydrylium Tetrafluoroborates **2**-BF₄ in Dichloromethane at 20 °C**

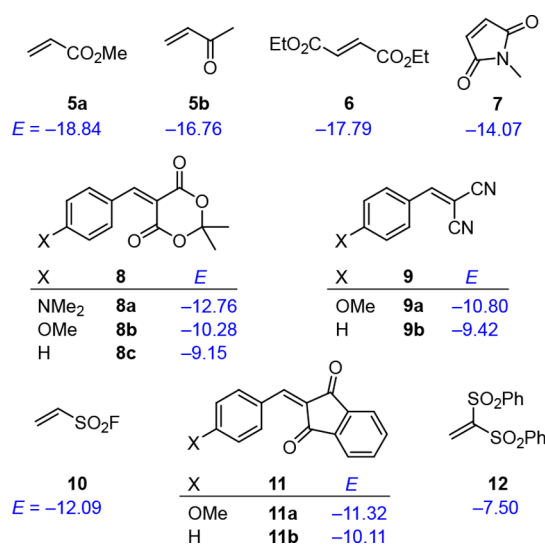
ArCHN ₂	N (s_N)	electrophile	k_2^{exptl} (M ⁻¹ s ⁻¹)
1a (X = H) ^a	9.35 (0.83)	2g	7.56×10^{-1}
		2e	1.19×10^2
		2d	5.80×10^2
		2b	6.85×10^3
		2a	1.45×10^5
		2f	8.46
1b (X = Br)	8.87 (0.82)	2e	3.66×10^1
		2d	3.02×10^2
		2c	4.59×10^2
		2b	2.51×10^3
		2f	6.21×10^{-1}
		2e	4.55
1c (X = CN)	7.66 (0.80)	2c	4.85×10^1
		2b	3.38×10^2
		2a	2.93×10^3
		2e	1.51
		2d	9.49
		2c	2.16×10^1
1d (X = NO ₂)	7.17 (0.83)	2e	1.26
		2d	1.26
		2c	2.16×10^1
		2b	1.26×10^2

^aData from ref 18.

with the Hammett substituent constants σ_p ($r^2 = 0.9909$).²¹ The resulting Hammett reaction constant of $\rho = -2.34$ will be discussed in the context of the kinetics of reactions of **1a–d** with Michael acceptors (see below).

Products of the Reactions of Aryldiazomethanes **1 with Michael Acceptors.** The reactions of the aryldiazomethanes **1a–d** with the Michael acceptors **5–12** (Chart 2) give either pyrazolines (from **5–7** and **10**) or nitrogen-free products (from **8–9** and **11–12**). As shown in Table 2, phenyldiazomethane (**1a**) reacts smoothly with methyl acrylate (**5a**)²² and methyl vinyl ketone (**5b**) at room temperature, affording the 5-phenyl- Δ^2 -pyrazolines **13a** and **13b** in 98% and

Chart 2. Michael Acceptors **5–12 and Their Electrophilicity Parameters E^a**



^aElectrophilicities E from refs 16 and 23.

68% isolated yield, respectively, via tautomerization of the initially formed Δ^1 -pyrazolines.

Under similar conditions, diethyl fumarate (**6**) undergoes 1,3-dipolar cycloadditions with aryldiazomethanes **1a** and **1b** to give Δ^1 -pyrazolines, which tautomerize with formation of 5-aryl- Δ^2 -pyrazolines **14a** as a single diastereomer or **14b** as a mixture of *cis/trans*-isomers.²⁴ The Δ^1 -pyrazoline initially formed from maleimide **7** and aryldiazomethane **1b** tautomerizes to give the Δ^2 -pyrazoline **16** (63%) with the aryl group in conjugation to the double bond. Ethenesulfonyl fluoride (ESF, **10**), employed as a second generation click reagent by Sharpless,^{23d,25} also undergoes smooth 1,3-dipolar cycloadditions with aryldiazomethanes **1a**, **1c**, and **1d** and yields the 5-aryl- Δ^2 -pyrazolines **15a–d** by subsequent

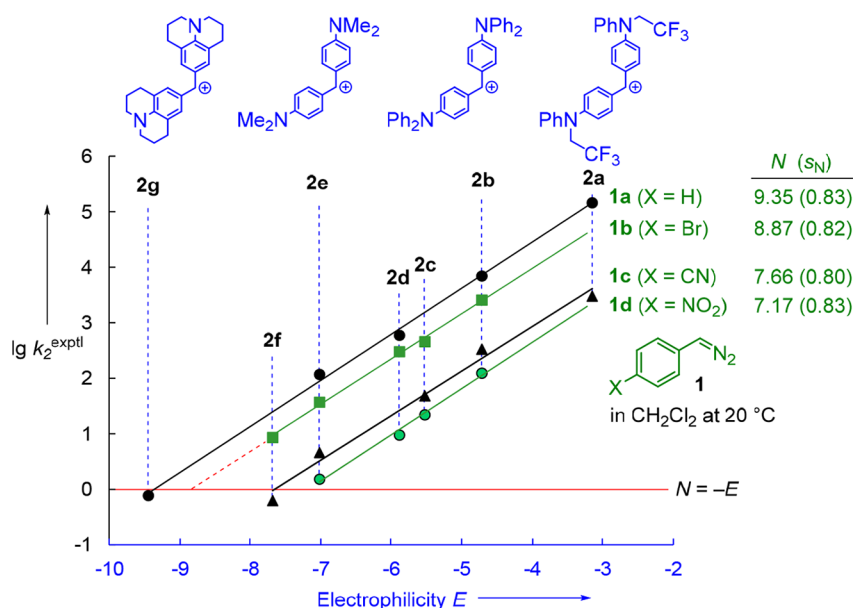
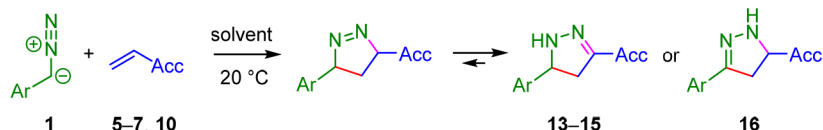


Figure 1. Plots of $\lg k_2^{\text{exptl}}$ for the reactions of the aryldiazomethanes **1a–d** with the reference electrophiles **2a–g** (in CH₂Cl₂ at 20 °C) versus their electrophilicity parameters E .

Table 2. Pyrazolines 13–16 Formed by Reactions of the Aryldiazomethanes 1a–d with the Dipolarophiles 5–7 and 10



1	Electrophile	Solvent	Products	Yield (%) ^a
1a	5a	toluene	(±)-13a	98
1a	5b	toluene	(±)-13b	68
1a	6	CH ₂ Cl ₂	(±)- <i>trans</i> -14a	48
1b	6	Et ₂ O	(±)- <i>trans</i> -14b + (±)- <i>cis</i> -14b	57 + 21
1b	7	CH ₂ Cl ₂	(±)-16	63
			X =	
1a	10	toluene	(±)-15a	93
1c	10	toluene	(±)-15c	79
1d	10	toluene	(±)-15d	99

^aYield of isolated products.

tautomerization. X-ray crystallography confirmed the structure of 15d (Figure 2).²⁶

The reaction of benzylidene Meldrum's acid derivative 8a with 2.5 equiv of phenyldiazomethane (1a) in dichloromethane at 0 °C furnished the cyclopropane (±)-17 in 62% yield (Scheme 3). It is likely that the 1,3-dipolar cycloaddition of 1a with 8a initially leads to pyrazoline F, in analogy to the reactions in Table 2. Subsequent migration of the electron-rich *p*-(dimethylamino)phenyl group and extrusion of molecular nitrogen generates the Michael acceptor G, which undergoes another cycloaddition with a second equivalent of diazoalkane 1a to deliver pyrazoline H. Finally, loss of N₂ from H generates the spirocycle (±)-17, which was purified by column chromatography and isolated as a racemate of a single diastereomer, which was identified by X-ray single crystal structure analysis (Figure 3). We did not search for other diastereomers in the mother liquors and have not explored the origin of the high stereoselectivity of the reaction of G with 1a.

Styrene derivatives 18a,c were obtained through the reactions of 1a,c with bis(phenylsulfonyl)ethene 12 (Figure 4a). Monitoring the reaction of 1c with 12 in CDCl₃ at ambient temperature by ¹H NMR spectroscopy shows the initial formation of 5-aryl-Δ¹-pyrazoline 19 within several seconds (Figure 4b).²⁷ The rate of this reaction is too fast to be followed by NMR spectroscopy, but could be determined

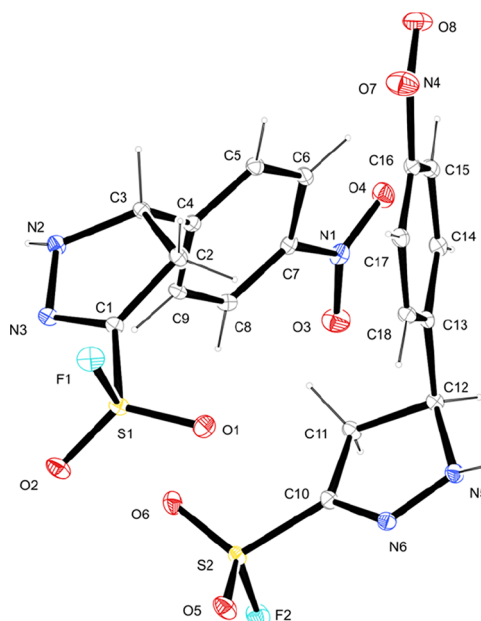


Figure 2. Crystal structure of (±)-15d (ellipsoids are shown on 50% probability level at *T* = 100 K).

Scheme 3. Reaction of Arylidene Meldrum's Acid 8a with Phenylhydrazomethane 1a and Proposed Mechanism for the Formation of (±)-17

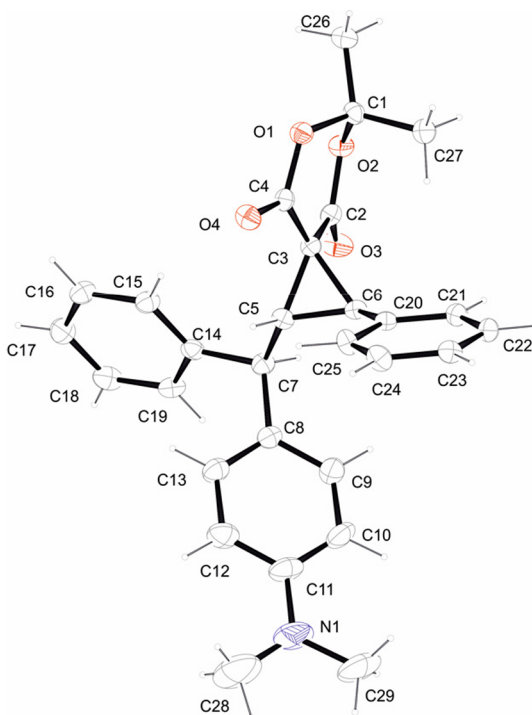
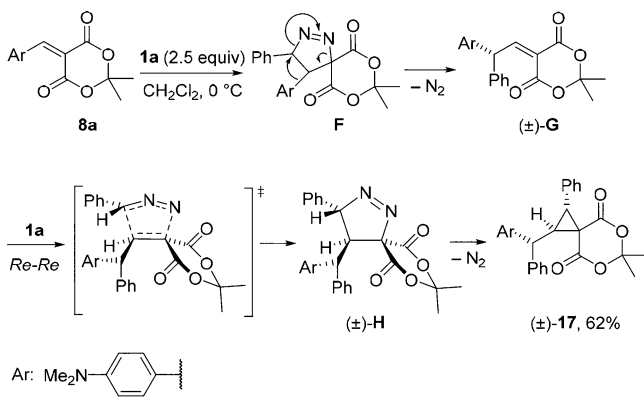


Figure 3. Crystal structure of (±)-17 (ellipsoids are shown on 50% probability level at $T = 100$ K).

by UV-vis spectrometry (see below). As shown by the ^1H NMR spectra in Figure 4b, **19** undergoes a quick N_2 elimination accompanied by hydrogen shift²⁸ and is completely converted into the 1,1-(bis-sulfonyl)-3-aryl-propene **20** within 2 h.²⁹ On a longer time scale, hydrogen migration converts **20** into **18c**, which was characterized by single crystal X-ray crystallography (Figure 4c).

Benzylidenemalononitrile (**9b**) reacts with phenylhydrazomethane (**1a**) in dichloromethane with formation of *trans*-2,3-diphenylcyclopropane **21**³⁰ (Scheme 4). The *trans*-configuration (that is, the C_2 symmetry) of **22**, which was obtained from **1a** and benzylidene-indane-1,3-dione (**11b**), was derived from the identical ^{13}C NMR chemical shifts of the carbonyl groups and the AA'BB' system in the ^1H NMR spectrum for the four aromatic protons of the indan-1,3-dione moiety. Though Schuster and co-workers observed the formation of Δ^1 -pyrazolines by the reactions of diazomethane

with **9b** or **11b** in diethyl ether at -45 and -10 °C, respectively,³¹ it is not certain that **21** and **22** are also formed through initial 1,3-dipolar cycloadditions, because the Δ^1 -pyrazoline from **9b** with phenylhydrazomethane (**1a**) was calculated to be an endergonic species (see below).

Kinetics of the Reactions of Aryldiazomethanes with Michael Acceptors. The kinetics of the reactions of aryldiazomethanes **1a–d** with various Michael acceptors from Chart 2 were followed by UV-vis spectroscopy using the methods described previously.¹⁶ Generally, pseudo-first-order conditions were employed. In most cases the dipolarophiles were used in excess (>10 equiv) over **1** and the kinetics were measured by following the decay of the absorbances of the phenyldiazomethanes **1** (295–380 nm, Chart 1). In the reactions with the colored electrophiles **8**, **9**, and **11**, compounds **1** were used in excess, however. The rates of the latter reactions were derived from the time-dependent absorbances of the styrene-chromophore in **8**, **9**, and **11**.

As illustrated for the reaction of **1b** with **10** in Figure 5, the pseudo-first order rate constants k_{obs} were obtained by least-squares fitting of the exponential function $A_t = A_0 \exp(-k_{\text{obs}}t) + C$ to the time-dependent absorbance A_t of the minor compound. The pseudo-first-order rate constants k_{obs} were proportional to the concentrations of the major compounds as shown by the inset of Figure 5, and the slopes of the correlations k_{obs} (s^{-1}) vs the concentrations of the excess compounds gave the second-order rate constants k_2^{exptl} ($\text{M}^{-1} \text{s}^{-1}$) listed in Table 3.

If the reactions of the phenyldiazomethanes **1** with the acceptor substituted ethylenes **5–12** would proceed stepwise, with rate-determining formation of zwitterionic intermediates, as illustrated in Scheme 5, the observed rate constants should equal those calculated by eq 1 because only one new bond is formed in the rate-determining step, as in the reactions used for deriving the reactivity parameters E , N , and s_N .¹³

To examine this possibility, we have used eq 1 to calculate the second-order rate constants k_2^{calcd} for the formation of the zwitterionic intermediates depicted in Scheme 5 from the one-bond nucleophilicities N and s_N of the diazoalkanes **1** (Table 1) and the one-bond electrophilicities E of the Michael acceptors **5–12** (Chart 2). Table 3 shows that all rate constants k_2^{exptl} measured for the reactions of **1a–d** with **8b,c**, **9a**, **11a,b**, and **12** differ by less than a factor of 50 from the rate constants k_2^{calcd} calculated by eq 1, while k_2^{exptl} is much larger than k_2^{calcd} for reactions of **1a–c** with **5a**, **5b**, and **6**.

A graphical illustration of these relationships is presented in Figure 6, where the blue line represents k_2^{calcd} , calculated by eq 1 for the formation of zwitterions from **1a** ($N = 9.35$, $s_N = 0.83$) and the electrophiles **5–12** (E from Chart 2). The shaded area of Figure 6 shows that a fair agreement between k_2^{exptl} and k_2^{calcd} (deviation $<$ factor 50) holds for all reactions of phenyldiazomethane (**1a**) with Michael acceptors of $E > -11$. The kinetic data thus indicate that the strongest electrophiles of this series either react via zwitterionic intermediates or via nonsynchronous concerted reactions with transition states resembling zwitterions. Table 3 and Figure 6 furthermore show that the deviations between k_2^{exptl} and k_2^{calcd} increase with decreasing electrophilicities of the Michael acceptors. Whereas the small deviations ($<$ factor 100) between k_2^{exptl} and k_2^{calcd} in the right part of Figure 6 cannot reliably be interpreted,³² the large deviations on the left indicate the operation of a concerted mechanism, and the term $RT \ln(k_2^{\text{exptl}}/k_2^{\text{calcd}})$ can be considered as a measure for the

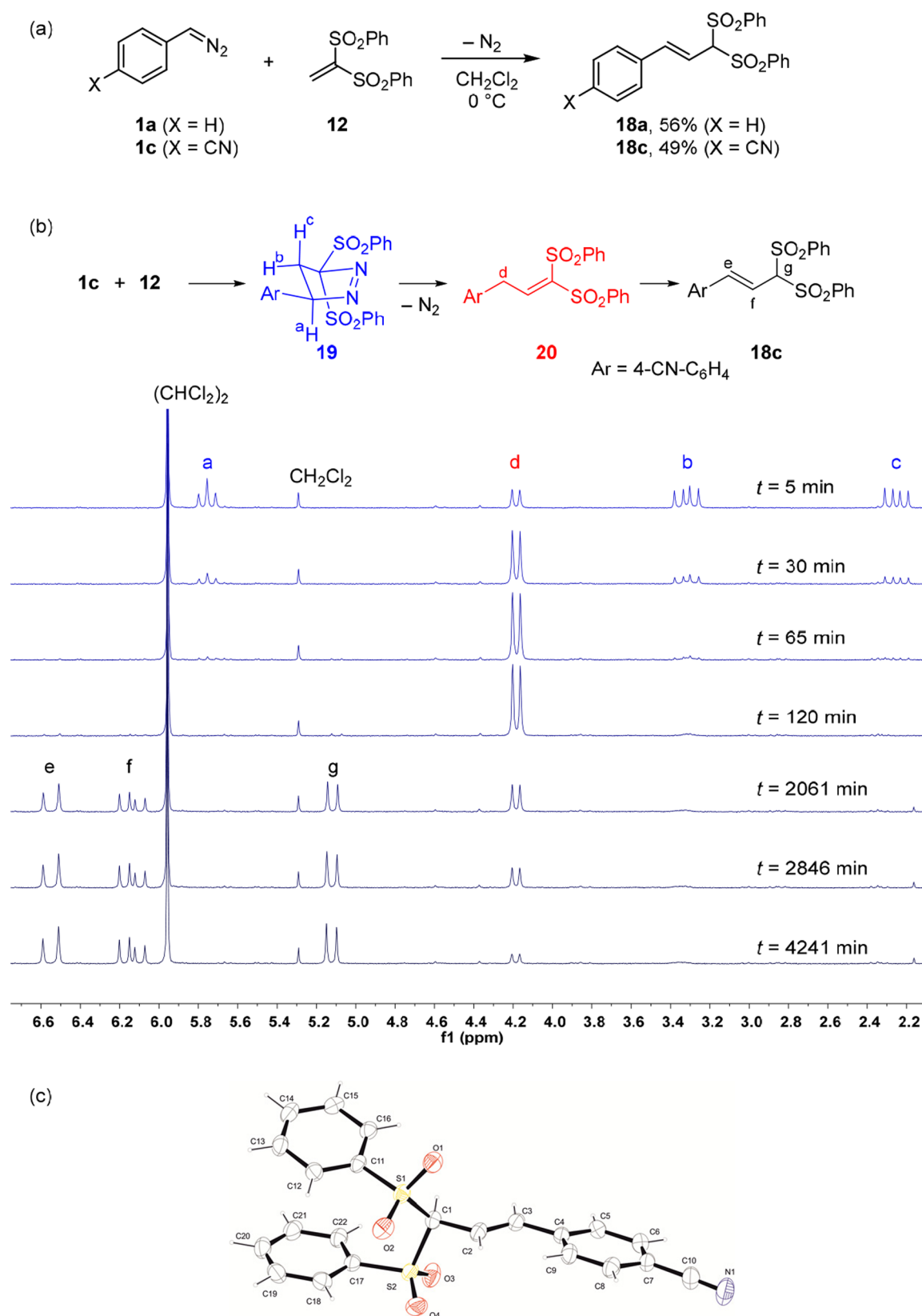
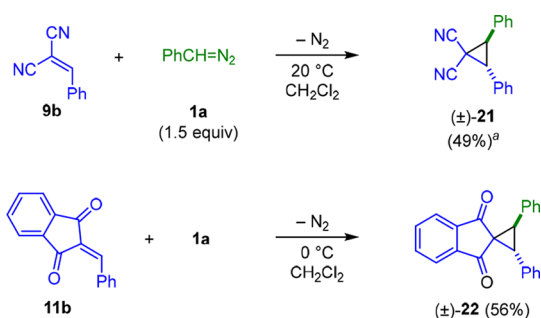


Figure 4. (a) Reactions of aryl diazomethanes **1a** and **1c** with bisulfone **12**. (b) Mechanism for the formation of **18c** monitored by ^1H NMR spectroscopy (200 MHz) of the reaction mixture [reaction of **1c** (0.10 M) with **12** (0.10 M) in CDCl_3 at 20°C using 1,1,2,2-tetrachloroethane (0.1 M) as an internal standard]. (c) Crystal structure of **18c** (ellipsoids are shown on 50% probability level at $T = 173\text{ K}$).

Scheme 4. Reactions of **9b** and **11b** with Phenyldiazomethane **1a**

^aDetermined by ¹H NMR spectroscopy (with 1,1,2,2-tetrachloroethane as an internal standard).

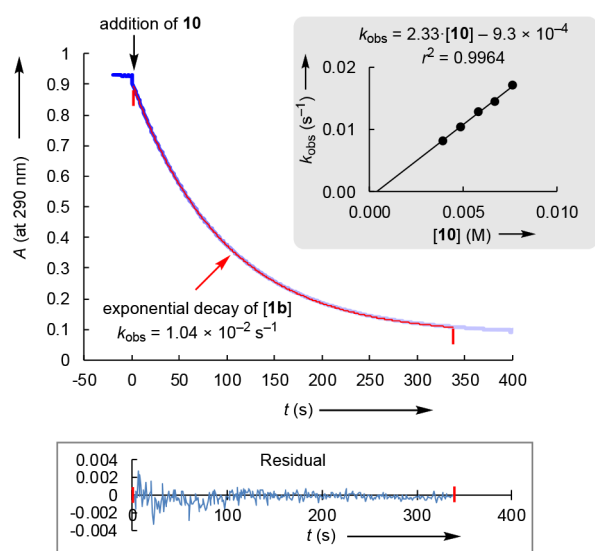


Figure 5. Monoexponential decay of the absorbance *A* (at 290 nm) vs time for the reaction of **10** (4.86×10^{-3} M) with **1b** (8.63×10^{-5} M) in CH_2Cl_2 at 20 °C. Inset: Correlation of k_{obs} vs the concentration of **10**.

energy of concert (eq 2) due to the stabilization of the transition state by the simultaneous formation of two new bonds (Figure 7).

In line with these interpretations, variation of the nucleophilic reactivities of the diazomethanes **1** affects the rates of the cycloadditions with the highly electrophilic Michael acceptors **12** and **10** to the same degree as the one-bond reactivities toward carbenium ion **2e** (Figure 8a). Comparable charge flows in the transition states of these reactions are thus indicated. The smaller dependence of the rate constants for the reactions with diethyl fumarate (**6**) on the nucleophilicities of the diazomethanes **1** is in accord with a high degree of concertedness of these reactions.

The same conclusion can also be drawn from the Hammett correlations shown in Figure 8b. The Hammett reaction constants for **12** ($\rho = -2.42$) and **10** ($\rho = -2.61$) are of similar magnitude as ρ for the reactions of **1** with the one-bond electrophile **2e** ($\rho = -2.34$). The reactions of aryldiazomethanes with diethyl fumarate (**6**) in dichloromethane at 20 °C, on the other hand, show a significantly less negative reaction constant ($\rho = -1.58$) indicating a smaller degree of negative charge transfer in the transition states. A similar

Hammett reaction constant of $\rho = -1.30$ ³³ can be derived from the rate constants which Huisgen and Geittner reported for the reactions of eight ring-substituted aryldiazomethanes with ethyl acrylate in DMF at 25 °C.^{22a}

The dependence of rate constants on solvent polarity has often been used as a criterion to differentiate concerted cycloadditions from cycloadditions through zwitterionic intermediates.^{22b,34} Whereas [2 + 2] cycloadditions of tetracyanoethylene with enol ethers, which proceed via zwitterionic intermediates, are 3–4 orders of magnitude faster in acetonitrile than in cyclohexane,^{34,35} the solvent dependence of various Diels–Alder reactions of tetracyanoethylene is so small that there are no significant correlations with any of the known solvent polarity parameters.³⁶

Solvent dependences of the rates of 1,3-dipolar cycloadditions were reported to be generally rather small. While the rate constants for the reactions of phenyldiazomethane (**1a**) with ethyl acrylate increased by a factor of 2.4 from cyclohexane to acetonitrile at 25 °C and correlated fairly with Reichardt's E_T values,³⁷ the rates of the corresponding reactions with norbornene were almost independent of solvent polarity.^{22b}

Table 4 shows that the reactions of phenyldiazomethane (**1a**) with the Michael acceptors **6** and **9–12** proceed slightly faster in the polar solvents acetonitrile and DMSO than in dichloromethane or THF. Though **12**, the strongest electrophile of the investigated Michael acceptors, showed the largest, and **6**, the weakest among the investigated electrophiles, showed the smallest solvent dependence, Table 4 does not reveal a clear correlation between electrophilicity of the dipolarophile and the magnitude of the solvent effect.

Quantum Chemical Calculations of the Cycloadditions. Details of the reaction pathways for the reactions of phenyldiazomethane (**1a**) with selected electrophiles have been calculated using the same quantum chemical methods as in our recent quantitative analysis of ketone reactivity.³⁸ This involves geometry optimizations at the (U)B3LYP³⁹-D3/6-31+G(d,p)⁴¹ level of theory in combination with the polarizable continuum model (PCM) for dichloromethane and UA0 radii.⁴² Thermochemical corrections to Gibbs energies (Corr. ΔG) and enthalpy (Corr. ΔH) at 298.15 K have been calculated using the rigid rotor/harmonic oscillator model without any scaling. Single point calculations have also been performed for all stationary points at the PCM-(CH_2Cl_2 ,UA0)/(U)B2PLYP⁴³-D3/def2TZVPP⁴⁴ level in order to verify the validity of all mechanistic conclusions (see the Supporting Information). Given the slightly better agreement between experimentally measured Gibbs activation energies with those calculated at the PCM(CH_2Cl_2 ,UA0)/(U)B3LYP-D3/6-31+G(d,p) level used for geometry optimization, only the latter results will be discussed in the following.

Figure 9 compares the Gibbs energy profiles for the reactions of phenyldiazomethane (**1a**) with five representative electrophiles. The initially formed encounter complexes, which are minima in potential energy, are omitted in these energy profiles, as they are endergonic species ($\Delta_r G^0 > 0$) and do not affect the kinetics. In all five cases, concerted (3 + 2)-cycloadditions are calculated to be the minimum energy pathways with Gibbs energies of activation, which agree within 5 kJ mol⁻¹ with the experimental ΔG^\ddagger obtained by applying the experimental rate constants k_2 from Table 3 in the Eyring equation. The direct formation of the thermodynamically

Table 3. Second-Order Rate Constants of Reactions between Aryldiazomethanes (1a–d) and Michael Acceptors (5–12) in Dichloromethane at 20 °C

ArCHN ₂	electrophile	k_2^{exptl} (M ⁻¹ s ⁻¹)	k_2^{calcd} (M ⁻¹ s ⁻¹) ^a	$k_2^{\text{exptl}}/k_2^{\text{calcd}}$	$\Delta G_{\text{concert}}^{\ddagger}$ (kJ mol ⁻¹)
1a	5a	4.87×10^{-2}	1.33×10^{-8}	3.7×10^6	37
	5b	2.22×10^{-1}	7.07×10^{-7}	3.1×10^5	31
	6	4.05×10^{-1}	9.88×10^{-8}	4.1×10^6	37
	8a	3.33×10^{-1}	1.48×10^{-3}	2.3×10^2	– ^b
	8b	7.58	1.69×10^{-1}	4.5×10^1	– ^b
	8c	4.80×10^1	1.47	3.3×10^1	– ^b
	9a	1.51×10^{-2}	6.26×10^{-2}	2.4×10^{-1}	– ^b
	10	6.81	5.32×10^{-3}	1.3×10^3	17
	11a	2.38×10^{-1}	2.32×10^{-2}	1.0×10^1	– ^b
	11b	1.45	2.34×10^{-1}	6.2	– ^b
	12	1.48×10^3	3.43×10^1	4.3×10^1	– ^b
1b	6	2.34×10^{-1}	4.85×10^{-8}	4.8×10^6	37
	7	8.46×10^{-1c}	5.45×10^{-5}	1.6×10^4	24
	10	2.33	2.29×10^{-3}	1.0×10^3	17
	12	6.59×10^2	1.33×10^1	5.0×10^1	– ^b
1c	6	3.87×10^{-2}	7.87×10^{-9}	4.9×10^6	38
	10	1.83×10^{-1}	2.86×10^{-4}	6.4×10^2	16
	12	4.56×10^1	1.34	3.4×10^1	– ^b
1d	7	1.74×10^{-2}	1.87×10^{-6}	9.3×10^3	22
	10	5.82×10^{-2}	8.25×10^{-5}	7.1×10^2	16
	12	2.16×10^1	5.32×10^{-1}	4.1×10^1	– ^b

^aCalculated by eq 1 with N and s_N from Table 1 and E from Chart 2. ^bToo small to be significant (see text). ^cDetermined by ¹H NMR spectroscopy.

Scheme 5. Stepwise 1,3-Dipolar Cycloadditions of Aryldiazomethanes with Acceptor-Substituted Ethylenes

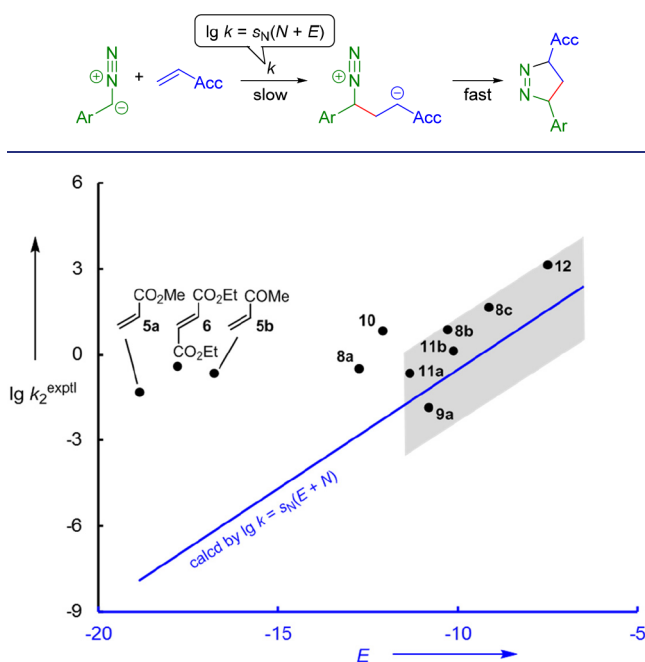


Figure 6. Correlation of $\lg k_2^{\text{exptl}}$ for the reactions between the Michael acceptors 5–12 and phenyldiazomethane (1a) versus the electrophilicity parameters E of the Michael acceptors.

favorable cyclopropanes (+ N₂) from the reactants generally requires higher activation energies. This suggests that also in those reactions listed in Table 3, where pyrazoline formation was not observed as in the reactions with 5a, 10, and 12, Δ^1 -pyrazolines are the initially formed products, which may undergo subsequent reactions.

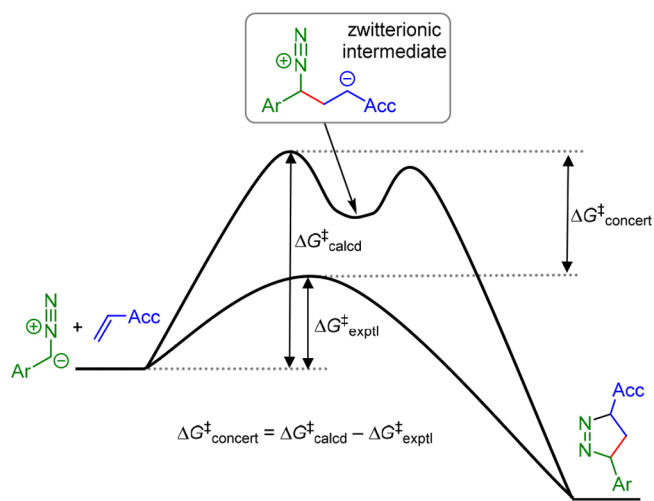


Figure 7. Comparison of measured activation Gibbs energies $\Delta G_{\text{exptl}}^{\ddagger}$ with $\Delta G_{\text{calcd}}^{\ddagger}$ calculated for the formation of zwitterions from E , N , and s_N by eq 1.

The calculated high Gibbs energy of the Δ^1 -pyrazoline from 1a and 9a indicates, however, that in this case conversion of the cycloadduct into the isolated cyclopropane and not the 1,3-dipolar cycloaddition may be rate-determining. This interpretation is supported by the observation that 9a is the only Michael acceptor which is below the calculated line in Figure 6. The excellent agreement between the measured rate constants for the reaction of 1a with 9a and that calculated for the 1,3-dipolar cycloaddition in Figure 9 indicates, on the other hand, that the barrier for nitrogen expulsion from the corresponding Δ^1 -pyrazoline cannot be much higher than that for retroaddition.

As shown by the geometrical parameters in Figure 10, the development of the new C–N bond lags far behind that of the

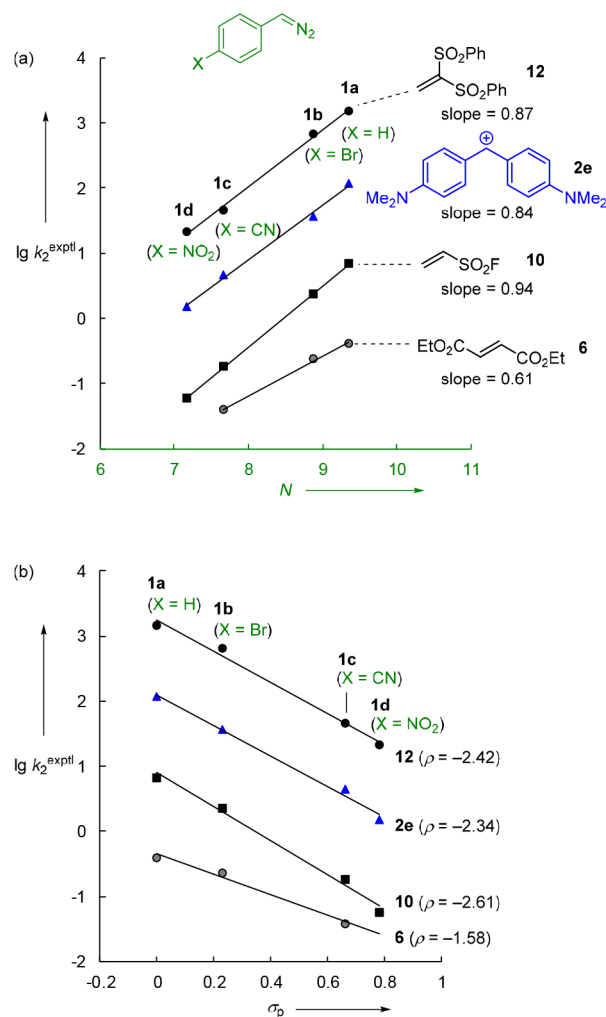


Figure 8. Correlation of $\lg k_2^{\text{exptl}}$ for the reactions of the electrophiles 2e, 6, 10, and 12 with the aryl diazomethanes 1a–d (from Tables 1 and 3) versus (a) the nucleophilicity parameters N of aryl diazomethanes (from Table 1) and (b) Hammett substituent constants σ_p (from ref 21) for 1a–d.

new C–C bond in all transition states, whereas both bonds have almost equal lengths in the resulting Δ^1 -pyrazolines. Figure 10 furthermore shows that the atomic distances in the two developing new bonds differ much more in the transition states of the highly electrophilic dipolarophiles ($\Delta = 0.5\text{--}0.7 \text{ \AA}$ for $E > -11$) than in the transition state for the reaction with methyl acrylate (5a, $\Delta = 0.3 \text{ \AA}$) for which a high degree of concertedness was derived from the kinetic data in Figure 6. This conclusion is confirmed by the relative bond orders (% E_V) and the amount of charge transfer from nucleophilic

diazomethane to electrophilic dipolarophile in the transition states (Figure 10). The latter parameter increases from $-0.2 e$ in the transition state of 5a to $-0.43 e$ in the most asynchronous transition state for 8c.

Though the data in Figure 10 are in line with highly unsymmetrical transition states in the reactions of phenyldiazomethane (1a) with highly electrophilic dipolarophiles, the question arises, how the concerted 1,3-dipolar cycloaddition mechanisms, derived from the quantum chemical calculations, concur with the zwitterion-like transition states derived from the kinetic data in Figure 6. Figure 9 shows that, on their way to cyclopropanes, the reactions of 1a with 8c ($E = -9.15$) or 12 ($E = -7.50$) initially yield zwitterions over barriers which are only 7 and 17 kJ mol^{-1} higher than the barriers for the concerted reactions, indicating that in the case of strong electrophiles ($E > -11$) concerted and stepwise cycloadditions proceed over comparable barriers. Obviously the interaction between the reaction centers at the “long” new bonds is so weak that the energy of the transition state is hardly affected. As a consequence, the one-bond nucleophilicities of the diazomethanes (N, s_N) and the one-bond-electrophilicities of the dipolarophiles (E) are suitable to calculate the rates of such cycloadditions by eq 1.

Following the distortion interaction analysis of 1,3-dipolar cycloadditions by Houk et al. and by Bickelhaupt et al.,¹⁰ we dissected the reaction barriers of the five reactions in Figure 9 into the distortion energies for deforming the two reactants into their transition state geometries and the interaction energies of the two distorted reactants when brought together into the transition state structure. As this procedure is based on single point energy calculations in the absence of thermal corrections, the resulting reaction barriers given in Figure 11 are much lower than the Gibbs energies reported in Figure 9. In agreement with earlier results by Houk and Ess for the reaction of methyl acrylate (5a) with diazomethane,^{10b} we found that, in the highly concerted cycloaddition of 1a with 5a ($E = -18.84$), the electrophile distortion energy is much smaller (27 kJ mol^{-1}) than that for the diazoalkane (69 kJ mol^{-1}). As the transition states become more unsymmetrical, the distortion energies of the electrophilic alkene grow and the distortion energies of the nucleophilic 1,3-dipole shrink with the consequence that, for the four highly unsymmetrical cycloadditions in Figure 11, the 1,3-dipole distortion energies are only slightly larger (in the case of 8c even smaller) than the dipolarophile distortion energies. According to this treatment, the higher reactivities of the more electrophilic dipolarophiles are predominantly due to the higher interaction energies.

Quantum Chemical Analysis of the Subsequent Reactions of the Δ^1 -Pyrazolines. As described in the subsection “Products of the Reactions of Aryldiazomethanes 1 with Michael Acceptors”, the initially generated Δ^1 -pyrazolines

Table 4. Second-Order Rate Constants k_2^{exptl} of the Reactions between Phenyldiazomethane (1a) and Michael Acceptors (6, 9–12) in Different Solvents at 20 °C

solvent	ϵ_r^a	$E_T(30)^a$	k_2^{exptl} ($\text{M}^{-1} \text{s}^{-1}$)				
			6 ($E = -17.79$)	10 ($E = -12.09$)	9a ($E = -10.80$)	11b ($E = -10.11$)	12 ($E = -7.50$)
DMSO	46.45	45.1	2.16	32.0	1.16×10^{-1}	7.63	8.00×10^3
CH_3CN	35.94	45.6		13.5	5.27×10^{-2}	3.18	
CH_2Cl_2	8.93	40.7	4.05×10^{-1}	6.81	1.51×10^{-2}	1.45	1.48×10^3
THF	7.58	37.4	4.08×10^{-1}	3.03		1.00	6.21×10^2

^aRelative permittivity (ϵ_r) and $E_T(30)$ were taken from ref 37.

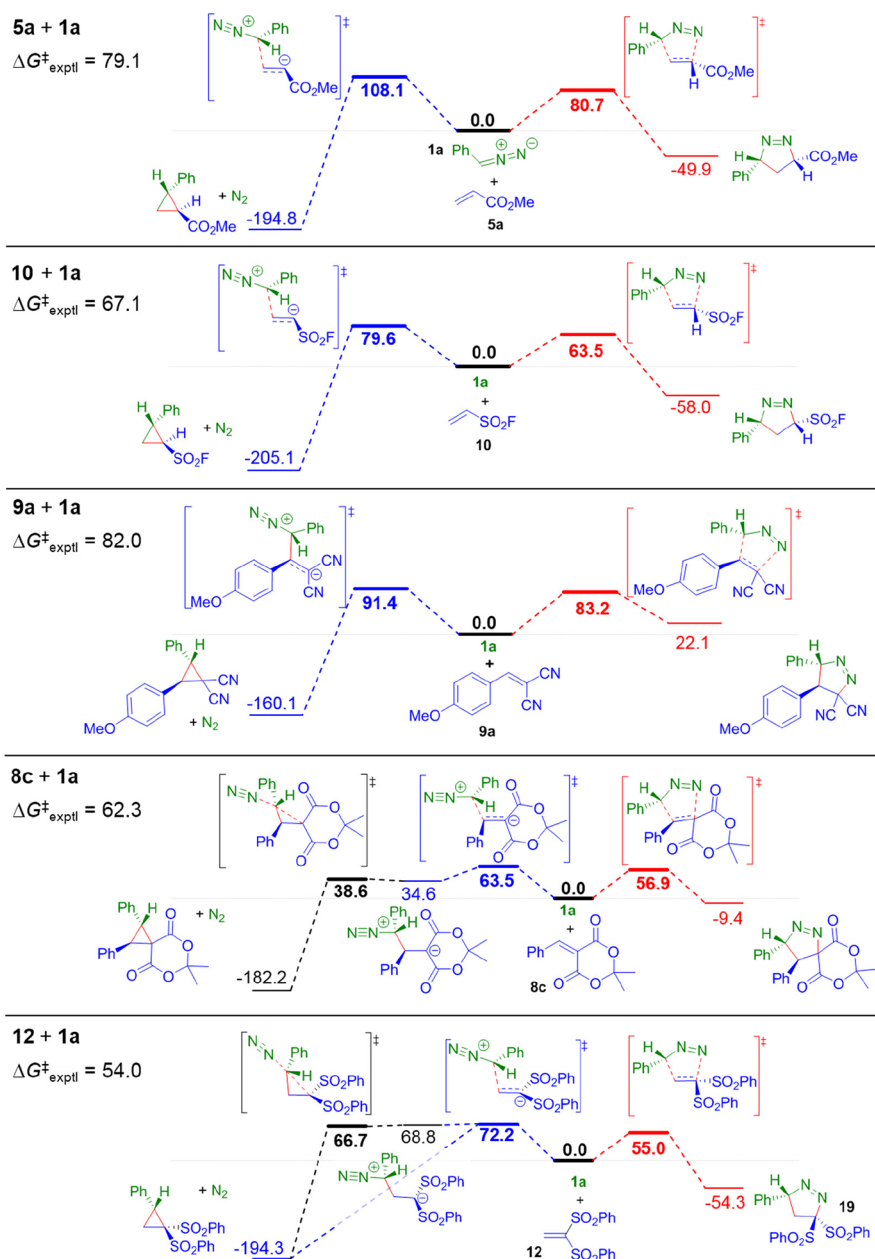


Figure 9. Energy profiles ($\Delta G_{\text{sol}}^{\ddagger}$, in kJ mol^{-1}) for the reactions of 5a, 10, 9a, 8c, and 12 with 1a calculated at the PCM(UA0,CH₂Cl₂)/(U)B3LYP-D3/6-31+G(d,p) level of theory.

were never isolated from the reactions of the aryldiazomethanes **1** with the Michael acceptors **5–12**. The isolated products were either Δ^2 -pyrazolines or nitrogen-free products.

Calculation of the relative stabilities of the pyrazoline tautomers obtained from **1a** and methyl acrylate (**5a**) and ESF (**10**) showed that the Δ^1 -pyrazolines are, indeed, the least stable tautomers (Scheme 6). However, according to Table 2, generally not the most stable tautomers with phenyl in conjugation with the endocyclic double bond were isolated but the tautomers with the acceptor group in conjugation with the double bond (exception: the bicyclic cycloadduct from maleimide **7**). Obviously, it is the higher acidity of the proton in α -position to the acceptor group that controls the mode of tautomerization.

As discussed above, according to Figure 9, Δ^1 -pyrazolines should be the initial reaction products in all investigated cases.

The formation of the cyclopropanes **21** and **22** (described in Scheme 4) may, therefore, proceed via retroaddition of the initially formed Δ^1 -pyrazolines to give the starting materials, which subsequently proceed to the cyclopropanes over the higher barriers on the left side of Figure 9. This pathway appears feasible, in particular for the reaction of **1a** with **9a**, since in this case the corresponding Δ^1 -pyrazoline is an endergonic adduct according to Figure 9.

Alternatively, the cyclopropanes may be formed through the direct conversion of the Δ^1 -pyrazolines. Figure 12 shows a possible transition state for such a transformation and also rationalizes the transformation of the Δ^1 -pyrazoline **19** into the bisulfonylethene **20**. Elongation of both C–N bonds leads to an activated complex ($\Delta G^{\ddagger} = 75.3 \text{ kJ mol}^{-1}$) on a flat surface, which may transform into N₂ complexes of a 1,3-zwitterion, an oxathiolane, or a cyclopropane, which are minima on the

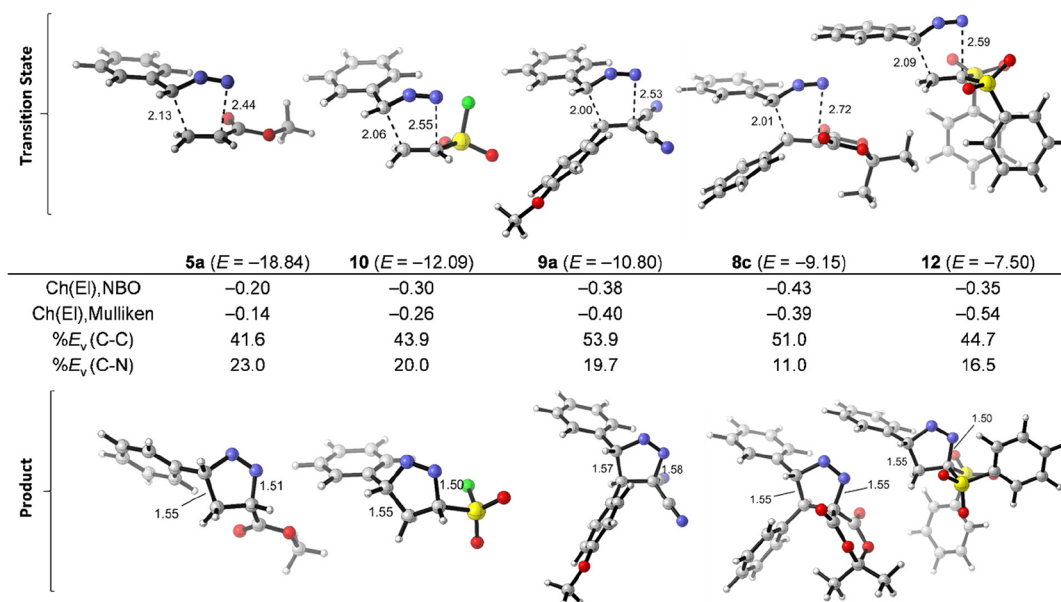


Figure 10. Charge on electrophilic dipolarophile [Ch(EI)] and percentage of evolution of the bond order (% E_v) in the transition states for the reactions of phenyldiazomethane (**1a**) with the electrophiles **5a**, **10**, **9a**, **8c**, and **12**. Charges (NBO6 and Mulliken) and % E_v (Wiberg indices) are calculated at the PCM(UA0,CH₂Cl₂)/(U)B3LYP-D3/6-31+G(d,p) level of theory. Distances are shown in Å.

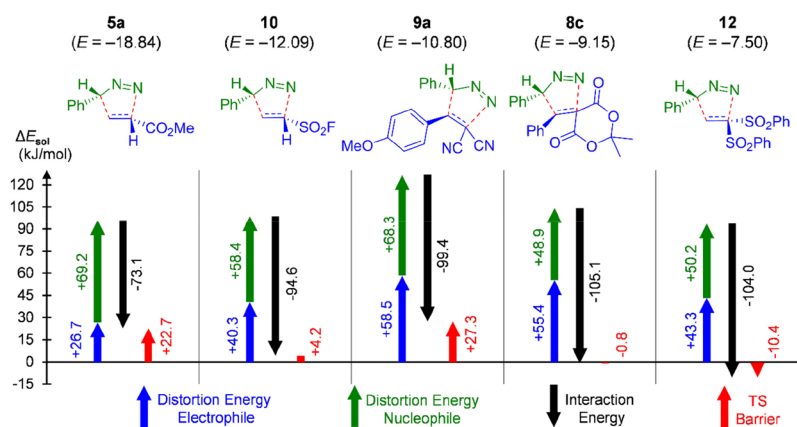
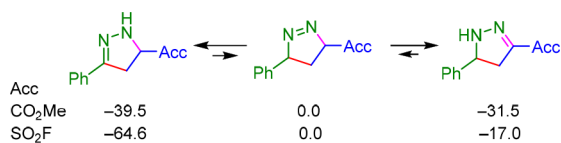


Figure 11. Distortion-interaction analysis (DIA, ΔE_{sol} , kJ mol⁻¹) for the reactions of phenyldiazomethane (**1a**) with the electrophiles **5a**, **10**, **9a**, **8c**, and **12**. DIA is performed at the PCM(UA0,CH₂Cl₂)/(U)B3LYP-D3/6-31+G(d,p) level of theory.

Scheme 6. Relative Stabilities (ΔG_{sol} , in kJ mol⁻¹) of the Tautomers Obtained from Reactions of Phenyldiazomethane (1a**) with Methyl Acrylate (**5a**) or ESF (**10**) Calculated at the PCM(UA0,CH₂Cl₂)/(U)B3LYP-D3/6-31+G(d,p) Level of Theory**



potential energy surface but not on the Gibbs energy surface and, therefore, immediately lose N₂. According to Figure 12, the barriers for the conversion of the oxathiolane (+78.6 kJ mol⁻¹) as well as of the cyclopropane intermediate (+163 kJ mol⁻¹) into **20** are higher than the barrier to form these intermediates from **19**. Since we did not observe any intermediates during conversion of **19** into **20** (Figure 4), we have to conclude that the alkene **20** is exclusively formed via the 1,3-zwitterion route shown in red in Figure 12. The

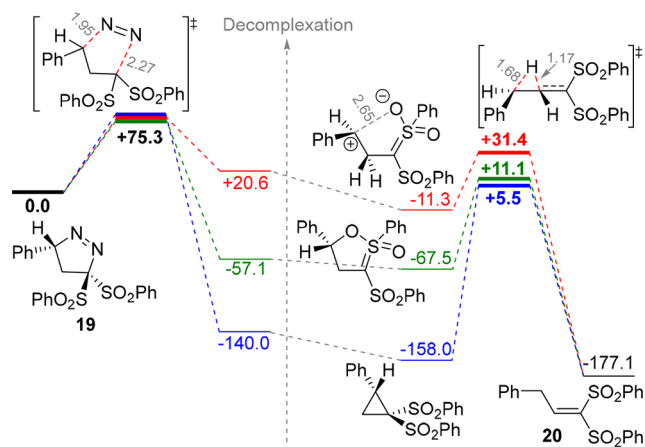


Figure 12. Energy profiles (ΔG_{sol} , kJ mol⁻¹) for the conversion of **19** into **20** (N₂ elimination accompanied by H shift) calculated at the PCM(UA0,CH₂Cl₂)/(U)B3LYP-D3/6-31+G(d,p) level of theory. Distances are shown in Å.

untypically high barrier for 1,2-hydride migration in the intermediate 1,3-zwitterion to give **20** can be assigned to the nonbonding interactions of the formal carbocation center with one of the sulfonyl oxygen atoms.

An analogous concerted extrusion of N₂ may account for the formation of the cyclopropanes **21** and **22** from **9b** and **11b**, respectively (Scheme 4).

CONCLUSION

The differentiation between concerted and stepwise processes has intrigued chemists for many years. In 1962, Doering and Roth used the term “No-mechanism” for so-called “thermoreorganization” reactions like the Diels–Alder and Cope and Claisen rearrangements, in which no involvement of intermediates was detectable.⁴⁵ A common rationale for such pericyclic reactions was provided in 1969 by Woodward and Hoffman’s orbital symmetry rules.⁴⁶ In his seminal 1984 article entitled “Multibond Reactions Cannot Normally Be Synchronous”, Dewar argued that even concerted cycloadditions proceed via transition states resembling intermediate biradicals or zwitterions.⁴⁷ Alabugin and co-workers demonstrated that the diradical/zwitterion dichotomy also applies to cycloaromatization reactions.⁴⁸ In this Article, we have introduced a linear free energy approach to measure the energy of concert, i.e., the difference between the activation energies of concerted 1,3-dipolar cycloadditions and of the corresponding stepwise processes via zwitterions.

We have shown that aryldiazomethanes undergo concerted, nonsynchronous 1,3-dipolar cycloadditions with electron-deficient CC-double bonds to give Δ^1 -pyrazolines, which are subsequently transformed into Δ^2 -pyrazolines, cyclopropanes, or substituted ethylenes. The direct formation of cyclopropanes from the reactants involves higher barriers and does not usually take place. Though the transformation of the Δ^1 -pyrazolines into cyclopropanes may proceed via nitrogen extrusion from the Δ^1 -pyrazolines and formation of intermediate 1,3-zwitterions, as illustrated in Figure 12, retroaddition with regeneration of the reactants and subsequent reaction over the higher barriers as shown on the left side of Figure 9 cannot generally be excluded.

The excellent agreement between experimental activation energies and quantum-chemically calculated values at the PCM(UA0,CH₂Cl₂)/(U)B3LYP-D3/6-31+G(d,p) level of theory for the cycloadditions shown in Figure 9 confirms the high reliability of the employed polarizable continuum model (PCM) to consider solvation. Charge densities and geometrical parameters of the transition states depicted in Figure 10 indicate that the nonsynchronicity of the cycloadditions increases with increasing electrophilicity of the acceptor-substituted ethylenes. Figure 6 shows that the measured rate constants for the cycloadditions of phenyldiazomethane (**1a**) with highly reactive Michael acceptors ($E > -11$ in Chart 2) are almost identical to those calculated by eq 1 from the one-bond nucleophilicities N and s_N of **1a** (Table 1) and the one-bond electrophilicities E of **5–12** (compiled with many other E parameters in a freely accessible online database¹⁴). This agreement indicates that the Gibbs activation energies for the concerted nonsynchronous cycloadditions of the highly electrophilic dipolarophiles closely resemble those for hypothetical stepwise cycloadditions via zwitterionic intermediates and that in these cases the formation of the new C–N bond cannot contribute significantly to the stabilization of the transition state of the concerted processes. The last two

examples in Figure 9 confirm the similar magnitude of the Gibbs activation energies for the concerted cycloadditions and the formation of zwitterions from the strong electrophiles **8c** and **12**. On the other hand, Figure 6 illustrates that less electrophilic dipolarophiles (such as, for example, methyl acrylate **5a**) react much faster with phenyldiazomethane (**1a**) than calculated by eq 1, and the ratio $k_2^{\text{exptl}}/k_2^{\text{calcd}}$ is suggested as a measure for concertedness (eq 2, Figure 7).

Correlations between measured rate constants and LUMO energies exist only for narrow subgroups of Michael acceptors sharing structural similarity at the site of nucleophilic attack. This is seen for the terminally unsubstituted electrophiles (**5a**, **5b**, **10**, and **12**) or for the aryldiene Meldrum’s acid derivatives (**8a–8c**) in Figure 13a. For a larger set of electrophiles,

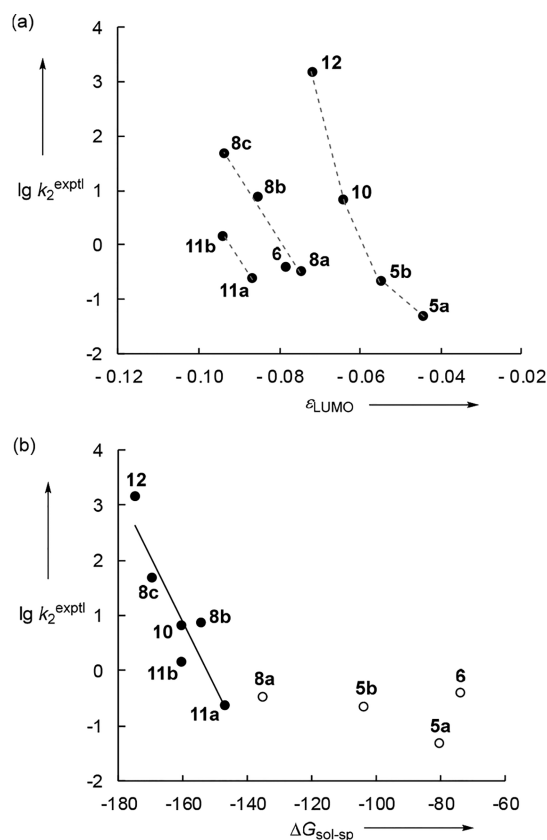


Figure 13. Second-order rate constants $\lg k_2^{\text{exptl}}$ for the reactions of **1a** with diverse electrophiles (from Table 3) correlated with (a) quantum-chemically calculated LUMO energies (ϵ_{LUMO} in Hartree, from ref 16) and (b) methyl anion affinities $\Delta G_{\text{sol-sp}}$ (in kJ mol^{-1} , from ref 16, correlation line refers to electrophiles of $E > -11$ in Chart 2. Data for **9a** excluded because formation of the Δ^1 -pyrazoline is not rate-determining, see main text.

however, neither the LUMO energies (Figure 13a) nor the global (ω) or the local (ω_β) Parr electrophilicity index serve as reliable descriptors of their reactivities (see the Supporting Information).

Figure 13b shows, however, that the cycloaddition rate constants of the highly electrophilic Michael acceptors (that is, those with $E > -11$ in Chart 2) correlate with their quantum-chemically calculated methyl anion affinities ($\Delta G_{\text{sol-sp}}$). This is a consequence of the correlation between cycloaddition rate constants and electrophilicities E of these Michael acceptors shown in Figure 6 and the previously reported linear

correlation between the electrophilicities E of a large variety of Michael acceptors and their calculated methyl anion affinities.¹⁶ As the correlation between the rate constants for the 1,3-dipolar cycloadditions and electrophilicities E breaks down for weaker electrophiles (that is, **8a**, **5b**, **5a**, and **6** with $E < -11$, Figure 6) the cycloaddition rate constants for these electrophiles also do not correlate with the corresponding methyl anion affinities (Figure 13b). While the methyl anion affinities of **8a**, **5b**, **5a**, and **6** cover a range of 70 kJ mol⁻¹, the rate constants for the (3 + 2)-cycloadditions with **1a** vary only within 1 order of magnitude, in line with the smaller amount of charge transfer in the transition states of these reactions.

Though the empirical electrophilicity parameters E (according to eq 1) thus do not allow to rank cycloaddition rates of less electrophilic dipolarophiles, the possibility to predict absolute rate constants for highly asynchronous 1,3-dipolar cycloadditions from the reactivity parameters E , N , and s_N represents a new tool, and we are currently investigating the applicability of this approach to other types of 1,3-dipolar cycloadditions.

■ ASSOCIATED CONTENT

📄 Supporting Information

The Supporting Information is available free of charge on the ACS Publications website at DOI: 10.1021/jacs.8b09995.

Details of the product studies, X-ray structures of **15d**, **17**, and **18c**, kinetic experiments, computational analysis, and NMR spectra of all characterized compounds (PDF)

Coordinates of optimized structures (ZIP)

Crystallographic data for **15d** (tv444), **17** (vv089), and **18c** (uo090) (CIF)

■ AUTHOR INFORMATION

Corresponding Authors

*ofial@lmu.de

*zipse@cup.uni-muenchen.de

*herbert.mayr@cup.uni-muenchen.de

ORCID

Armin R. Ofial: 0000-0002-9600-2793

Hendrik Zipse: 0000-0002-0534-3585

Herbert Mayr: 0000-0003-0768-5199

Present Addresses

[‡]Q.C.: Novaled GmbH, 01307 Dresden, Germany.

[§]I.Z.: Merck KGaA, 64293 Darmstadt, Germany.

Author Contributions

[†]H.J. and Q.C. contributed equally to this work.

Notes

The authors declare no competing financial interest.

■ ACKNOWLEDGMENTS

Dedicated to Professor Kendall N. Houk on the occasion of his 75th birthday. We thank the Deutsche Forschungsgemeinschaft (SFB 749, Projects B1 and C6) for financial support and the Leibniz Supercomputing Centre (www.lrz.de) for generous allocation of computational resources.

■ REFERENCES

(1) (a) Huisgen, R. 1,3-Dipolar Cycloadditions. Past and Future. *Angew. Chem., Int. Ed. Engl.* **1963**, *2*, 565–598. (b) Huisgen, R. 1,3-Dipolar Cycloadditions – Introduction, Survey, Mechanism. In *1,3-*

Dipolar Cycloaddition Chemistry Vol. 1; Padwa, A., Ed.; Wiley: New York, 1984; Chapter 1, pp 1–176. (c) Wang, L.-J.; Tang, Y. Intermolecular 1,3-dipolar cycloadditions of alkenes, alkynes, and allenes. In *Comprehensive Organic Synthesis*, 2nd ed.; Knochel, P., Molander, G. A., Eds.; Elsevier: Amsterdam, 2014; Vol. 4, pp 1342–1383. (d) Menon, R. S.; Nair, V. Intramolecular 1,3-dipolar cycloadditions of alkenes, alkynes, and allenes. In *Comprehensive Organic Synthesis*, 2nd ed.; Knochel, P., Molander, G. A., Eds.; Elsevier: Amsterdam, 2014; Vol. 4, pp 1281–1341. (e) Huisgen, R. Steric course and mechanism of 1,3-dipolar cycloadditions. *Adv. Cycloaddit.* **1988**, *1*, 1–31. (f) Singh, M. S.; Chowdhury, S.; Koley, S. Progress in 1,3-dipolar cycloadditions in the recent decade: an update to strategic development towards the arsenal of organic synthesis. *Tetrahedron* **2016**, *72*, 1603–1644. (g) Hashimoto, T.; Maruoka, K. Recent Advances of Catalytic Asymmetric 1,3-Dipolar Cycloadditions. *Chem. Rev.* **2015**, *115*, 5366–5412. (h) Pellissier, H. Asymmetric 1,3-dipolar cycloadditions. *Tetrahedron* **2007**, *63*, 3235–3285.

(2) (a) Gothelf, K. V.; Jørgensen, K. A. Asymmetric 1,3-Dipolar Cycloaddition Reactions. *Chem. Rev.* **1998**, *98*, 863–910. (b) Chen, S.; Bacauanu, V.; Knecht, T.; Mercado, B. Q.; Bergman, R. G.; Ellman, J. A. New Regio- and Stereoselective Cascades via Unstabilized Azomethine Ylide Cycloadditions for the Synthesis of Highly Substituted Tropane and Indolizidine Frameworks. *J. Am. Chem. Soc.* **2016**, *138*, 12664–12670. (c) Mulzer, J. Natural Product Synthesis via 1,3-Dipolar Cycloadditions. In *Organic Synthesis Highlights*; Mulzer, J., Altenbach, H.-J., Braun, M., Krohn, K., Reissig, H.-U., Eds.; VCH: Weinheim, 1991; pp 77–95. (d) Döndas, H. A.; de Gracia Retamosa, M.; Sansano, J. M. Current Trends towards the Synthesis of Bioactive Heterocycles and Natural Products Using 1,3-Dipolar Cycloadditions with Azomethine Ylides. *Synthesis* **2017**, *49*, 2819–2851. (e) Mulzer, J. Selected diastereoselective reactions. Diastereoselective intra- and intermolecular 1,3-dipolar cycloadditions in natural product synthesis. In *Comprehensive Chirality*; Carreira, E. M., Yamamoto, H., Eds.; Elsevier: Amsterdam, 2012; Vol. 2, pp 525–562. (f) Padwa, A. Use of nitrogen and oxygen dipole ylides for alkaloid synthesis. *ARKIVOC* **2018**, 23–49.

(3) (a) Maggini, M.; Scorrano, G.; Prato, M. Addition of Azomethine Ylides to C₆₀: Synthesis, Characterization, and Functionalization of Fullerene Pyrrolidines. *J. Am. Chem. Soc.* **1993**, *115*, 9798–9799. (b) Hummelen, J. C.; Knight, B. W.; LePeq, F.; Wudl, F.; Yao, J.; Wilkins, C. L. Preparation and Characterization of Fulleroid and Methanofullerene Derivatives. *J. Org. Chem.* **1995**, *60*, 532–538. (c) Guldi, D. M.; Maggini, M.; Scorrano, G.; Prato, M. Intramolecular Electron Transfer in Fullerene/Ferrocene Based Donor-Bridge-Acceptor Dyads. *J. Am. Chem. Soc.* **1997**, *119*, 974–980. (d) Lutz, J.-F. 1,3-Dipolar Cycloadditions of Azides and Alkynes: A Universal Ligation Tool in Polymer and Materials Science. *Angew. Chem., Int. Ed.* **2007**, *46*, 1018–1025.

(4) (a) Kolb, H. C.; Finn, M. G.; Sharpless, K. B. Click Chemistry: Diverse Chemical Function from a Few Good Reactions. *Angew. Chem., Int. Ed.* **2001**, *40*, 2004–2021. (b) Kolb, H. C.; Sharpless, K. B. The growing impact of click chemistry on drug discovery. *Drug Discovery Today* **2003**, *8*, 1128–1137. (c) Amblard, F.; Cho, J. H.; Schinazi, R. F. Cu(I)-Catalyzed Huisgen Azide–Alkyne 1,3-Dipolar Cycloaddition Reaction in Nucleoside, Nucleotide, and Oligonucleotide Chemistry. *Chem. Rev.* **2009**, *109*, 4207–4220. (d) Kacprzak, K.; Skiera, I.; Piasecka, M.; Paryzek, Z. Alkaloids and Isoprenoids Modification by Copper(I)-Catalyzed Huisgen 1,3-Dipolar Cycloaddition (Click Chemistry): Toward New Functions and Molecular Architectures. *Chem. Rev.* **2016**, *116*, 5689–5743. (e) Belkheira, M.; El Abed, D.; Pons, J.-M.; Bressy, C. Chemoselective Organoclick–Click Sequence. *Synthesis* **2018**, *50*, 4254–4262.

(5) (a) Huisgen, R. On the Mechanism of 1,3-Dipolar Cycloadditions. A Reply. *J. Org. Chem.* **1968**, *33*, 2291–2297. (b) Houk, K. N.; Firestone, R. A.; Munchausen, L. L.; Mueller, P. H.; Arison, B. H.; Garcia, L. A. Stereospecificity of 1,3-Dipolar Cycloadditions of *p*-Nitrobenzoxitrile Oxide to *cis*- and *trans*-Dideuterioethylene. *J. Am. Chem. Soc.* **1985**, *107*, 7227–7228.

(6) For an alternative diradical pathway, see: Firestone, R. A. On the Mechanism of 1,3-Dipolar Cycloadditions. *J. Org. Chem.* **1968**, *33*, 2285–2290.

(7) Theories of 1,3-dipolar cycloaddition: (a) Sustmann, R. A simple model for substituent effects in cycloaddition reactions. I. 1,3-dipolar cycloadditions. *Tetrahedron Lett.* **1971**, *12*, 2717–2720. (b) Sustmann, R.; Trill, H. Substituent Effects in 1,3-Dipolar Cycloadditions of Phenyl Azide. *Angew. Chem., Int. Ed. Engl.* **1972**, *11*, 838–840. (c) Houk, K. N.; Yamaguchi, K. Theory of 1,3-Dipolar Cycloadditions. In *1,3-Dipolar Cycloaddition Chemistry*; Padwa, A., Ed.; Wiley: New York, 1984; Vol. 2; Chapter 13, pp 407–450.

(8) (a) Huisgen, R.; Mloston, G.; Langhals, E. The first two-step 1,3-dipolar cycloadditions: non-stereospecificity. *J. Am. Chem. Soc.* **1986**, *108*, 6401–6402. (b) Huisgen, R.; Mloston, G.; Langhals, E. The first two-step 1,3-dipolar cycloadditions: interception of intermediate. *J. Org. Chem.* **1986**, *51*, 4085–4087. (c) Baran, J.; Mayr, H. The First [4 + 3] Cycloaddition of a 1,3-Dipole with a 1,3-Diene. *J. Am. Chem. Soc.* **1987**, *109*, 6519–6521. (d) Baran, J.; Mayr, H. Mechanistic Impact of Oxime Formation Accompanying 1,3-Dipolar Cycloadditions of Nitrile Oxides. *J. Org. Chem.* **1989**, *54*, 5012–5016. (e) Baran, J.; Mayr, H. Competing [2 + 3] and [4 + 3] Cycloadditions of C,N-Diphenylnitron with 1,3-Dienes. Evidence for Thermally Non-equilibrated Intermediates. *J. Org. Chem.* **1989**, *54*, 5774–5783.

(9) (a) Houk, K. N. The Frontier Molecular Orbital Theory of Cycloaddition Reactions. *Acc. Chem. Res.* **1975**, *8*, 361–369. (b) Fleming, I. *Molecular Orbitals and Organic Chemical Reactions* (Student ed.); Wiley: Chichester, UK, 2009; pp 242–252. (c) Carey, F. A.; Sundberg, R. J. *Advanced Organic Chemistry—Part A: Structure and Mechanisms*, 5th ed.; Springer: New York, 2007; pp 873–883.

(10) (a) Ess, D. H.; Houk, K. N. Distortion/Interaction Energy Control of 1,3-Dipolar Cycloaddition Reactivity. *J. Am. Chem. Soc.* **2007**, *129*, 10646–10647. (b) Ess, D. H.; Houk, K. N. Theory of 1,3-Dipolar Cycloadditions: Distortion/Interaction and Frontier Molecular Orbital Models. *J. Am. Chem. Soc.* **2008**, *130*, 10187–10198. (c) Lan, Y.; Zou, L.; Cao, Y.; Houk, K. N. Computational Methods to Calculate Accurate Activation and Reaction Energies of 1,3-Dipolar Cycloadditions of 24 1,3-Dipoles. *J. Phys. Chem. A* **2011**, *115*, 13906–13920. (d) Bickelhaupt, F. M.; Houk, K. N. Analyzing Reaction Rates with the Distortion/Interaction-Activation Strain Model. *Angew. Chem., Int. Ed.* **2017**, *56*, 10070–10086.

(11) (a) van Zeist, W.-J.; Bickelhaupt, F. M. The activation strain model of chemical reactivity. *Org. Biomol. Chem.* **2010**, *8*, 3118–3127. (b) Fernández, I.; Bickelhaupt, F. M. The activation strain model and molecular orbital theory: understanding and designing chemical reactions. *Chem. Soc. Rev.* **2014**, *43*, 4953–4967.

(12) (a) Engels, B.; Christl, M. What Controls the Reactivity of 1,3-Dipolar Cycloadditions? *Angew. Chem., Int. Ed.* **2009**, *48*, 7968–7970. (b) Breugst, M.; Huisgen, R.; Reissig, H.-U. Regioselective 1,3-Dipolar Cycloaddition of Diazoalkanes with Heteroatom-Substituted Alkynes: Theory and Experiment. *Eur. J. Org. Chem.* **2018**, 2477–2485.

(13) (a) Mayr, H.; Bug, T.; Gotta, M. F.; Hering, N.; Irrgang, B.; Janker, B.; Kempf, B.; Loos, R.; Ofial, A. R.; Remennikov, G.; Schimmel, H. Reference Scales for the Characterization of Cationic Electrophiles and Neutral Nucleophiles. *J. Am. Chem. Soc.* **2001**, *123*, 9500–9512. (b) Lucius, R.; Loos, R.; Mayr, H. Kinetics of Carbocation Carbanion Combinations: Key to a General Concept of Polar Organic Reactivity. *Angew. Chem., Int. Ed.* **2002**, *41*, 91–95. (c) Mayr, H.; Kempf, B.; Ofial, A. R. π -Nucleophilicity in Carbon-Carbon Bond-Forming Reactions. *Acc. Chem. Res.* **2003**, *36*, 66–77. (d) Mayr, H.; Ofial, A. R. Kinetics of Electrophile-Nucleophile Combinations: A General Approach to Polar Organic Reactivity. *Pure Appl. Chem.* **2005**, *77*, 1807–1821. (e) Richter, D.; Hampel, N.; Singer, T.; Ofial, A. R.; Mayr, H. Synthesis and Characterization of Novel Quinone Methides: Reference Electrophiles for the Construction of Nucleophilicity Scales. *Eur. J. Org. Chem.* **2009**, 3203–3211. (f) Mayr, H.; Lakhdar, S.; Majji, B.; Ofial, A. R. A quantitative approach to nucleophilic organocatalysis. *Beilstein J. Org. Chem.* **2012**, *8*, 1458–1478. (g) Mayr, H. Reactivity Scales for Quantifying Polar

Organic Reactivity: The Benzhydrylium Methodology. *Tetrahedron* **2015**, *71*, 5095–5111. (h) Mayer, R. J.; Hampel, N.; Mayer, P.; Ofial, A. R.; Mayr, H. Synthesis, Structure and Properties of Amino-Substituted Benzhydrylium Ions – a Link Between Ordinary Carbocations and Neutral Electrophiles. *Eur. J. Org. Chem.* **2018**, DOI: 10.1002/ejoc.201800835.

(14) For a listing of nucleophilicity parameters N , s_N , and electrophilicity parameters E , see: <http://www.cup.uni-muenchen.de/oc/mayr/DBintro.html>.

(15) (a) Regitz, M. Diazoalkanes. In *1,3-Dipolar Cycloaddition Chemistry*; Padwa, A., Ed.; Wiley: New York, 1984; Vol. 1; Chapter 4, pp 393–558. (b) Aronoff, M. R.; Gold, B.; Raines, R. T. 1,3-Dipolar Cycloadditions of Diazo Compounds in the Presence of Azides. *Org. Lett.* **2016**, *18*, 1538–1541. (c) Gold, B.; Aronoff, M. R.; Raines, R. T. Decreasing Distortion Energies without Strain: Diazo-Selective 1,3-Dipolar Cycloadditions. *J. Org. Chem.* **2016**, *81*, 5998–6006.

(16) Allgäuer, D. S.; Jangra, H.; Asahara, H.; Li, Z.; Chen, Q.; Zipse, H.; Ofial, A. R.; Mayr, H. Quantification and Theoretical Analysis of the Electrophilicities of Michael Acceptors. *J. Am. Chem. Soc.* **2017**, *139*, 13318–13329.

(17) (a) Doering, W. v. E.; Roth, W. R.; Breuckmann, R.; Figge, L.; Lennartz, H.-W.; Fessner, W.-D.; Prinzbach, H. Verbotene Reaktionen. – [2 + 2]-Cycloreversion starrer Cyclobutane. *Chem. Ber.* **1988**, *121*, 1–9. (b) Hartnagel, M.; Grimm, K.; Mayr, H. Addition and Cycloaddition Reactions of Arenediazonium Ions with 1,3-Dienes: A Shift from a Concerted to a Stepwise Mechanism. *Liebigs Ann./Recueil* **1997**, 71–80. (c) Mayr, H.; Henninger, J. Kinetics of the [2⁺+4]-Cycloaddition Reactions of [1,3]-Dithian-2-ylidene Ions with 1,3-Dienes. *Eur. J. Org. Chem.* **1998**, 1919–1922. (d) Mayr, H.; Ofial, A. R.; Sauer, J.; Schmied, B. [2⁺+4] Cycloadditions of Iminium Ions - Concerted or Stepwise Mechanism of Aza Diels-Alder Reactions? *Eur. J. Org. Chem.* **2000**, 2013–2020. (e) Fichtner, C.; Mayr, H. Diels-Alder reactions of 1,1,3-triaryllallyl cations: Determination of the free energy of concert. *J. Chem. Soc., Perkin Trans. 2* **2002**, 1441–1444. (f) Kanzian, T.; Mayr, H. Electrophilic Reactivities of Azodicarboxylates. *Chem. - Eur. J.* **2010**, *16*, 11670–11677.

(18) Phenyl diazomethane (**1a**) has been characterized previously: Bug, T.; Hartnagel, M.; Schlierf, C.; Mayr, H. How Nucleophilic are Diazo Compounds? *Chem. - Eur. J.* **2003**, *9*, 4068–4076.

(19) (a) Streitwieser, A., Jr An Interpretation of the Reaction of Aliphatic Primary Amines with Nitrous Acid. *J. Org. Chem.* **1957**, *22*, 861–869. (b) Friedman, L. Carbonium Ion Formation From Diazonium Ions. In *Carbonium Ions Vol. II*; Olah, G. A., Schleyer, P. v. R., Eds.; Wiley-Interscience: New York, 1970; Chapter 16, pp 655–713. (c) Zollinger, H. *Diazo Chemistry II*; VCH: Weinheim, 1995; Chapter 7, pp 241–304.

(20) (a) Katz, C. E.; Ribelin, T.; Withrow, D.; Basseri, Y.; Manukyan, A. K.; Bermudez, A.; Nuera, C. G.; Day, V. W.; Powell, D. R.; Poutsma, J. L.; Aubé, J. Nonbonded, Attractive Cation- π Interactions in Azide-Mediated Asymmetric Ring Expansion Reactions. *J. Org. Chem.* **2008**, *73*, 3318–3327. (b) Gutierrez, O.; Aubé, J.; Tantilillo, D. J. Mechanism of the Acid-Promoted Intramolecular Schmidt Reaction: Theoretical Assessment of the Importance of Lone Pair-Cation, Cation- π , and Steric Effects in Controlling Regioselectivity. *J. Org. Chem.* **2012**, *77*, 640–647.

(21) Hansch, C.; Leo, A.; Hoekman, D. *Exploring QSAR: Hydrophobic, Electronic, and Steric Constants*; American Chemical Society: Washington, DC, 1995.

(22) (a) Huisgen, R.; Geittner, J. Kinetics of 1,3-Dipolar Cycloaddition Reactions of Aryl- and Diaryldiazomethanes. *Heterocycles* **1978**, *11*, 105–108. (b) Geittner, J.; Huisgen, R.; Reissig, H.-U. Solvent Dependence of Cycloaddition Rates of Phenyl diazomethane and Activation Parameters. *Heterocycles* **1978**, *11*, 109–112.

(23) (a) Allgäuer, D. S.; Mayr, H. Electrophilicities of 1,2-Disubstituted Ethylenes. *Eur. J. Org. Chem.* **2014**, 2956–2963. (b) Kaumanns, O.; Mayr, H. Electrophilicity Parameters of 5-Benzylidene-2,2-dimethyl-[1,3]dioxane-4,6-diones (Benzylidene Meldrum's Acids). *J. Org. Chem.* **2008**, *73*, 2738–2745. (c) Lemek, T.;

Mayr, H. Electrophilicity Parameters for Benzylidenemalononitriles. *J. Org. Chem.* **2003**, *68*, 6880–6886. (d) Chen, Q.; Mayer, P.; Mayr, H. Ethenesulfonyl Fluoride (ESF): The Most Perfect Michael Acceptor Ever Found? *Angew. Chem., Int. Ed.* **2016**, *55*, 12664–12667. (e) Berger, S. T. A.; Seeliger, F. H.; Hofbauer, F.; Mayr, H. Electrophilicity Parameters for 2-Benzylidene-indan-1,3-diones - a systematic extension of the benzhydrylium based electrophilicity scale. *Org. Biomol. Chem.* **2007**, *5*, 3020–3026. (f) Asahara, H.; Mayr, H. Electrophilicities of Bissulfonyl Ethylenes. *Chem. - Asian J.* **2012**, *7*, 1401–1407.

(24) The relative configurations of **14a** and **14b** were determined by NMR spectroscopy. See the [Supporting Information](#).

(25) (a) Krutak, J. J.; Burpitt, R. D.; Moore, W. H.; Hyatt, J. A. Chemistry of ethenesulfonyl fluoride. Fluorosulfonylethylation of organic compounds. *J. Org. Chem.* **1979**, *44*, 3847–3858. (b) Dong, J.; Krasnova, L.; Finn, M. G.; Sharpless, K. B. Sulfur(VI) Fluoride Exchange (SuFEx): Another Good Reaction for Click Chemistry. *Angew. Chem., Int. Ed.* **2014**, *53*, 9430–9448. (c) Zheng, Q.; Dong, J.; Sharpless, K. B. Ethenesulfonyl Fluoride (ESF): An On-Water Procedure for the Kilogram-Scale Preparation. *J. Org. Chem.* **2016**, *81*, 11360–11362.

(26) Crystallographic data have been deposited with the Cambridge Crystallographic Data Centre [CCDC 1862870 (**15d**), 1862871 (**17**), 1862872 (**18c**)]. These supplementary crystallographic data can be obtained free of charge from The Cambridge Crystallographic Data Centre via www.ccdc.cam.ac.uk/data_request/cif.

(27) Yoshimatsu, M.; Kawahigashi, M.; Honda, E.; Kataoka, T. A convenient synthesis of alkylnylpyrazoles. *J. Chem. Soc., Perkin Trans. 1* **1997**, 695–700.

(28) (a) McGreer, D. E.; Wu, W. S. Pyrazolines. VII. Concerning the formation of olefins from the pyrolysis of pyrazolines. *Can. J. Chem.* **1967**, *45*, 461–468. (b) McGreer, D. E.; Masters, I. M. E. Pyrazolines X. Kinetics for the pyrolysis of some deuterated 1-pyrazolines in solution. *Can. J. Chem.* **1969**, *47*, 3975–3978.

(29) The vinylic proton of **20** (not shown in [Figure 4b](#)) resonates as a triplet ($J = 7.9$ Hz) at δ 7.82 ppm (see [Supporting Information](#)).

(30) The relative configuration of **21** was determined based on its reported NMR spectra and crystal structure, see: Lin, S.; Li, M.; Dong, Z.; Liang, F.; Zhang, J. Hypervalent iodine(III)-mediated cyclopropa(e)nation of alkenes/alkynes under mild conditions. *Org. Biomol. Chem.* **2014**, *12*, 1341–1350.

(31) Kisch, H.; Polansky, O. E.; Schuster, P. Thermisch instabile Δ^1 -Pyrazoline durch Reaktion von Diazomethan mit Olefinen bei tiefen Temperaturen. *Tetrahedron Lett.* **1969**, *10*, 805–808.

(32) Since the three-parameter [eq 1](#), which covers a reactivity range of approximately 40 orders of magnitude, provides rate constants only with an accuracy of a factor of 100, deviations of this order of magnitude cannot reliably be interpreted. See also: Mayr, H. Reply to T.W. Bentley: Limitations of the $s(E+N)$ and Related Equations. *Angew. Chem., Int. Ed.* **2011**, *50*, 3612–3618.

(33) Calculated from rate constants in Table 1 of ref [22a](#) and Hammett σ -parameters from ref [21](#).

(34) See ref [1b](#), pp 76–90.

(35) (a) Steiner, G.; Huisgen, R. Tetracyanoethylene and Enol Ethers. Dependence of Cycloaddition Rate on Solvent Polarity. *J. Am. Chem. Soc.* **1973**, *95*, 5056–5058. (b) Huisgen, R. Tetracyanoethylene and Enol Ethers. A Model for 2 + 2 Cycloadditions via Zwitterionic Intermediates. *Acc. Chem. Res.* **1977**, *10*, 117–124.

(36) (a) Brown, P.; Cookson, R. C. Kinetics of Addition of Tetracyanoethylene to Anthracene and Bicyclo[2,2,1]heptadiene. *Tetrahedron* **1965**, *21*, 1977–1991. (b) Konovalov, A. I.; Breus, J. P.; Sharagin, I. A.; Kiselev, V. D. Solvation Effects in the Diels-Alder Reactions of 4-Phenyl-1,2,4-triazoline-3,5-dione with Anthracene and trans,trans-1,4-Diphenyl-1,3-butadiene. *J. Org. Chem. USSR* **1979**, *15*, 315–320. (c) Sauer, J.; Sustmann, R. Mechanistic Aspects of Diels-Alder Reactions: A Critical Survey. *Angew. Chem., Int. Ed. Engl.* **1980**, *19*, 779–807.

(37) Reichardt, C.; Welton, T. *Solvents and Solvent Effects in Organic Chemistry*, Fourth ed.; Wiley-VCH: Weinheim, 2011; pp 455–461.

(38) Li, Z.; Jangra, H.; Chen, Q.; Mayer, P.; Ofial, A. R.; Zipse, H.; Mayr, H. Kinetics and Mechanism of Oxirane Formation by Darzens Condensation of Ketones: Quantification of the Electrophilicities of Ketones. *J. Am. Chem. Soc.* **2018**, *140*, 5500–5515.

(39) Becke, A. D. Density-functional thermochemistry. III. The role of exact exchange. *J. Chem. Phys.* **1993**, *98*, 5648–5652.

(40) (a) Grimme, S. Semiempirical GGA-Type Density Functional Constructed with a Long-Range Dispersion Correction. *J. Comput. Chem.* **2006**, *27*, 1787–1799. (b) Grimme, S.; Antony, J.; Ehrlich, S.; Krieg, H. A consistent and accurate ab initio parametrization of density functional dispersion correction (DFT-D) for the 94 elements H-Pu. *J. Chem. Phys.* **2010**, *132*, 154104. (c) Wagner, J. P.; Schreiner, P. R. London Dispersion in Molecular Chemistry—Reconsidering Steric Effects. *Angew. Chem., Int. Ed.* **2015**, *54*, 12274–12296.

(41) (a) Ditchfield, R.; Hehre, W. J.; Pople, J. A. Self-Consistent Molecular-Orbital Methods. IX. An Extended Gaussian-Type Basis for Molecular-Orbital Studies of Organic Molecules. *J. Chem. Phys.* **1971**, *54*, 724–728. (b) Krishnan, R.; Binkley, J. S.; Seeger, R.; Pople, J. A. Self-consistent molecular orbital methods. XX. A basis set for correlated wave functions. *J. Chem. Phys.* **1980**, *72*, 650–654.

(42) (a) Cancès, E.; Mennucci, B.; Tomasi, J. A new integral equation formalism for the polarizable continuum model: Theoretical background and applications to isotropic and anisotropic dielectrics. *J. Chem. Phys.* **1997**, *107*, 3032–3041. (b) Tomasi, J.; Mennucci, B.; Cammi, R. Quantum Mechanical Continuum Solvation Models. *Chem. Rev.* **2005**, *105*, 2999–3094. (c) Mayer, R. J.; Tokuyasu, T.; Mayer, P.; Gomar, J.; Sabelle, S.; Mennucci, B.; Mayr, H.; Ofial, A. R. Solvation Accounts for the Counter-Intuitive Nucleophilicity Ordering of Peroxide Anions. *Angew. Chem., Int. Ed.* **2017**, *56*, 13279–13282.

(43) Grimme, S. Semiempirical hybrid density functional with perturbative second-order correlation. *J. Chem. Phys.* **2006**, *124*, 034108.

(44) (a) Weigend, F.; Ahlrichs, R. Balanced basis sets of split valence, triple zeta valence and quadruple zeta valence quality for H to Rn: Design and assessment of accuracy. *Phys. Chem. Chem. Phys.* **2005**, *7*, 3297–3305. (b) Weigend, F. Accurate Coulomb-fitting basis sets for H to Rn. *Phys. Chem. Chem. Phys.* **2006**, *8*, 1057–1065.

(45) Doering, W. v. E.; Roth, W. R. The Overlap of Two Allyl Radicals or a Four-Centered Transition State in the Cope Rearrangement. *Tetrahedron* **1962**, *18*, 67–74.

(46) Woodward, R. B.; Hoffmann, R. The Conservation of Orbital Symmetry. *Angew. Chem., Int. Ed. Engl.* **1969**, *8*, 781–853.

(47) Dewar, M. J. S. Multibond Reactions Cannot Normally Be Synchronous. *J. Am. Chem. Soc.* **1984**, *106*, 209–219.

(48) (a) Peterson, P. W.; Mohamed, R. K.; Alabugin, I. V. How to Lose a Bond in Two Ways – The Diradical/Zwitterion Dichotomy in Cycloaromatization Reactions. *Eur. J. Org. Chem.* **2013**, 2505–2527. (b) dos Passos Gomes, G.; Alabugin, I. V. Drawing Catalytic Power from Charge Separation: Stereoelectronic and Zwitterionic Assistance in the Au(I)-Catalyzed Bergman Cyclization. *J. Am. Chem. Soc.* **2017**, *139*, 3406–3416.